CROSS-CORRELATION BETWEEN THE 170 GHz SURVEY MAP AND THE *COBE* DIFFERENTIAL MICROWAVE RADIOMETER FIRST-YEAR MAPS

Ken Ganga[a], Ed Cheng[b], Stephan Meyer[c] & Lyman Page[a]

[a]Joseph Henry Laboratories, Jadwin Hall, Princeton University, Princeton, NJ 08544

[b]Laboratory for Astronomy and Solar Physics, NASA Goddard Space Flight Center, Greenbelt, MD 20771

[c]Massachusetts Institute of Technology, Department of Physics, Room 20F-001, Cambridge, MA 02139

Abstract

This paper describes results of a cross-correlation between the 170 GHz partial-sky survey, made with a 3°.8 beam balloon-borne instrument and the *COBE* DMR 'Fit Technique' reduced galaxy all-sky map with a beam of 7°. The strong correlation between the data sets implies that the observed structure is consistent with thermal variations in a 2.7K emitter. We describe a number of tests of the correlation: 1) A χ^2 analysis applied to the correlation function rules out the assumption that there is no structure in either of the two maps. 2) A second test shows that if the DMR map has structure but the 170 GHz map does not, the probability of obtaining the observed correlation is small. 3) Further analyses support the assumption that both maps have structure and that the 170 GHz—DMR cross-correlation is consistent with the analogous DMR correlation function. 4) Maps containing various combinations of noise and Harrison-Zel'dovich power spectra are simulated and correlated to reinforce the result. Because these two experiments use completely different observing strategies, observing frequencies, and data reduction methods, the correlation provides compelling evidence that both instruments have observed fluctuations consistent with anisotropies in the cosmic microwave background.
Subject heading: cosmic microwave background

I. Introduction

The recent discovery of anisotropy in the cosmic microwave background (CMB) by the differential microwave radiometer (DMR) aboard NASA's *COBE* satellite (Bennett *et al.*, 1992, hereafter B92, Smoot *et al.*, 1992, hereafter S92 and Wright *et al.*, 1992) provides strong evidence for primordial structure in the CMB. Supporting this claim is an exhaustive battery of checks for possible systematic effects and foreground sources (B92, Kogut *et al.*, 1992).

The 170 GHz survey map (Meyer *et al.*, 1991), covering roughly one third the sky with an angular resolution of 3°.8, is an independent set of data with enough sensitivity to confirm the *COBE* DMR detection. We find significant cross-correlation between the survey map and the DMR 'Fit Technique' reduced galaxy map (hereafter simply DMR; See B92, §5.2). Since the 170 GHz map is made with a different observing strategy, uses different data reduction methods, and is sensitive to different galactic contaminants, the correlation supports the argument for the cosmic origin of the structure seen in the DMR maps. Because of the higher frequency and finer angular resolution, these data may be used to set bounds on the spectrum of the fluctuations, probe the angular dependence of the anisotropy down to $3^\circ.8$, and find a more precise value of Q_{rms-PS}; future work will address these questions specifically (Bond *et al.*, 1993).

II. The Data

The 170 GHz survey experiment and instrument are described in Meyer *et al.*, 1991, Page, 1990, Page *et al.*, 1991, and Page *et al.*, 1993. The data were collected in a single balloon flight in October 1989. The map used in this analysis has had an offset, a dipole, and a model of the galaxy subtracted in a five parameter fit of the data with $|b| > 15^\circ$. The best fit dipole is in the direction of $\alpha = 169^\circ$ and $\delta = -7^\circ.3$ ($l = 267^\circ$, $b = 49^\circ$) in the solar rest frame. A dipole magnitude of 3.25 mK (3.36 mK plus corrections for the earth's motion) is used to calibrate the data. To model the galaxy, we use the *IRAS* 100 μm map with a model of zodiacal dust emission removed (Boulanger, 1989) and convolved with the survey map beam. For the purpose of cross-correlation, we again consider only data for which $|b| > 15^\circ$, where the contribution from the interstellar dust emission is small. The auto-correlation function of the dust removed indicates that interstellar emission is insignificant. A similar analysis with the survey's highest frequency channel confirms this. We are confident that galactic emission accounts for less than 200 $(\mu\mathrm{K})^2$ in the first bin of the correlation function.

The DMR data used here is the 'Fit Technique' reduced galaxy map described in B92, §2 with a 15° galactic cut. The reduced galaxy map and the 15° galactic cut are used to minimize the influence of the galaxy at small galactic latitudes, as demonstrated in Figure 2 of S92. The total weight of this map is 0.118 $(\mu\mathrm{K})^{-2}$, roughly twice that of the 170 GHz map.

To compare the 170 GHz and DMR data sets, we make a new map called "masked DMR." It is a partial sky map made with only those DMR pixels within the 170 GHz survey coverage. The total weight of the masked DMR map is 0.024 $(\mu\mathrm{K})^{-2}$, about half that of the 170 GHz map.

III. Analysis

The correlation function is given by $C(\theta_A) = (\Gamma_A)^{-1} \sum_{i,j\in A} t_i t'_j w_i w'_j$, where $\Gamma_A = \sum_{i,j\in A} w_i w'_j$, t_i and w_i are the temperature and weight of pixel i in one map, t'_j and w'_j are the temperature and weight of pixel j in the second map, and the sum is taken over all pixels i and j such that the angle between pixel i and pixel j is θ_A. When the auto-correlation is formed, $t'_j = t_j$ and $w'_j = w_j$. The bin size used here for the correlation function is $180^\circ/32 = 5^\circ.63$.

The statistical distribution of $t_i t_j$ for a single pair of pixels is shown in Appendix B to be approximated by a zero-order, modified Bessel function of the second kind. The value of $C(\theta)$ is the weighted mean of data drawn from these distributions; by the central limit theorem, the distribution of $C(\theta)$ is sufficiently Gaussian for our purposes (Bond, 1992. See also Cayón *et al.*, 1991).

The covariance matrix of the correlation function used here, the diagonal terms of which are the variances σ_A^2 of the correlation function, is (see Appendix A)

$$\Sigma_{AB} = \frac{\delta_{AB}}{\Gamma_A} + \frac{1}{\Gamma_A \Gamma_B} \sum_{i,j \in A} w_i w'_j \left(t'_j \sum_{l:i,l \in B} w'_l t'_l + t_i \sum_{k:j,k \in B} w_k t_k \right), \tag{1}$$

$$\begin{aligned} \Sigma_{AB} =& \frac{\delta_{AB}}{\Gamma_A}\left(1 + \frac{\Gamma_A^*}{\Gamma_A}\right) + \frac{1}{\Gamma_A \Gamma_B}\left(\sum_{i,j \in A} w_i w'_j \left(t'_j \sum_{l:i,l \in B} w'_l t'_l + t_i \sum_{k:j,k \in B} w_k t_k \right) \right. \\ & \left. + \sum_{j \in 1 \cap 2} w_j^* \sum_{i:i,j \in A} w_i t_i \sum_{l:j,l \in B} w'_l t'_l + \sum_{i \in 1 \cap 2} w_i^* \sum_{j:i,j \in A} w'_j t'_j \sum_{k:i,k \in B} w_k t_k \right). \end{aligned} \tag{2}$$

Equation 1 applies to a cross-correlation, while Equation 2 is used for a correlation between two maps in which overlapping pixel values are the same in both maps. Equation 2 thus applies to an auto-correlation, for which all pixels in one map have the same values as their counterparts in the second map, as well as to a correlation between a map and a subset of the same map, such as the correlation between the masked DMR map and the full-sky DMR map. $\sum_{j \in 1 \cap 2} x_j^*$ is the sum of x_j over the common coverage of the two maps and Γ_A^* is the Γ_A one gets for the auto-correlation of the common coverage of the two maps. As outlined in the appendix, these expressions are the covariances if one assumes that both maps have structure in them. If both maps are assumed to have no signal other than noise, only the first (diagonal) terms should be used.

Figure 1 shows the correlation between the 170 GHz survey map and the DMR map along with that of the masked DMR map and the full-sky DMR map. The errors shown are obtained under the assumption that neither map has any real structure. If this assumption is valid, $\chi_\nu^2 = (1/N_{bins}) \sum_A C(A)/\sigma^2(A)$ is about one. The actual value is 5.2. This indicates that the probability of getting the observed level cross-correlation if both maps have only Gaussian noise in them is less than .5%. Simulations confirm this conclusion.

We simulate maps with nothing but Gaussian noise following the 170 GHz map weights and correlate them with maps with nothing but noise following the DMR map weights. The thinnest of the three shaded swaths centered on zero in Figure 2 represents the 1 σ range of results for these correlations, again demonstrating that the observed correlation is quite improbable if both maps simply contain pure noise. From this we infer that our assumption was incorrect and that there must be structure in at least one of the maps.

Next, we assume that the DMR map has structure, but that the 170 GHz map does not. In this case we must use the first two of the three terms in the covariance matrix of Equation 1 (we associate the DMR map with the primed weight and temperature values). Because the covariance matrix is no longer diagonal, the simple χ^2 analysis used previously is not valid, since different bins in the correlation function are now correlated. In order to apply a χ^2 test, we find the matrix $\mathbf{T}$ which diagonalizes the covariance matrix $\mathbf{\Sigma}$ and transform to get a new, diagonal covariance matrix $\mathbf{\Sigma}' = \mathbf{T}^{-1}\mathbf{\Sigma}\mathbf{T}$, and a new correlation function $\mathbf{C}' = \mathbf{TC}$. The errors in the new correlation function are, as before, the square roots of the diagonal terms in the new covariance matrix. In this new space, since the covariance matrix is diagonal, the errors in separate bins of the correlation function are independent and we can do a χ^2 test. We find a χ^2_ν of 5.7 for the transformed 170 GHz—DMR cross-correlation, once again indicating that our assumption is incorrect — there must be structure in the survey map. This is the primary conclusion in Meyer *et al.*, 1991. Figure 2 reinforces this result. The second of the three bands centered around zero represents the 1 σ range of results of correlations between the simulated maps with nothing but noise and the real DMR map. Again we see that the observed correlation is quite unlikely if it is assumed that the 170 GHz map has only noise, although because of the covariances a quantitative comparison of the real and simulated correlation functions is not possible.

This leads us to the assumption that there is structure in both maps, and requires use of the full covariance matrix for the correlation function. Transforming again as outlined above, we get a χ^2_ν of 2.6, indicating that the function is still inconsistent with zero, this time in accordance with our assumption.

Are the two correlation functions in Figure 1 consistent with each other? To address this question we calculate the full covariance matrices for both correlation functions and transform both according to the transformation that diagonalizes the 170 GHz—DMR correlation function covariance matrix. We now have two transformed correlation functions and corresponding covariance matrices. The covariance matrix corresponding to the 170 GHz—DMR correlation function is diagonal, while the off diagonal terms in the covariance matrix associated with the masked DMR—full-sky DMR correlation are small. We then define a statistic similar to the χ^2:

$$\xi^2_\nu = \frac{\xi^2}{\nu} = \frac{1}{N_{bins}} \sum_A \frac{\left(C'_1(A) - C'_2(A)\right)^2}{\sigma'_1(A)^2 + \sigma'_2(A)^2},$$

where $C'_j(A)$ and $\sigma'_j(A)$ are the value and error of the j^{th} transformed correlation function at bin A. ξ^2 is χ^2 distributed; if the statistic is small, the two functions are consistent with each other. We find $\xi^2_\nu = 0.6$, indicating that there is a 90-95% chance of getting a higher ξ^2. Transforming so that the masked DMR—full-sky DMR covariance matrix is diagonalized again yields $\xi^2_\nu = 0.6$. As a further test of the consistency, Figure 2 shows that the observed cross-correlation is consistent with the 1 σ range of results obtained when simulated Harrison-Zel'dovich skies with $Q_{rms-PS} = 17$ μK and 170 GHz map noise are correlated with the same underlying skies and DMR map noise. A quantitative comparison of the actual cross-correlation and the simulations would be misleading, in this case because the simulations contain "cosmic variance" in the covariance, while the real cross-correlation function does not (see Appendix A).

The widest path about zero in Figure 2 is the result of the same simulated Harrison-Zel'dovich skies with the 170 GHz sky coverage and noise cross-correlated with the DMR map. It indicates that even if two maps have underlying structure with the same rms temperature variations, they still do not correlate as well as the 170 GHz and DMR maps.

For a strong correlation, the structure in the two maps must have the same phase and amplitude relation.

We are indebted to Dick Bond, Steve Boughn and David Cottingham for enlightening discussions on statistics and map making. Appendix A grew out of notes Steve Boughn shared with us. We would also like to thank the *COBE* team, especially Chuck Bennett, Gary Hinshaw, Charley Lineweaver and George Smoot for independently checking the results presented in Figure 1 and thoroughly reading an earlier manuscript. In addition, Gary Hinshaw checked our galaxy subtraction.

This work was supported by the NSF and NASA Grant NAGW-1841.

Appendix A: Covariance Matrix of the Correlation Function

The standard expression for the covariance matrix of the correlation function $C(\theta_A)$ (see § III) is $\Sigma_{AB} = \langle (C(\theta_A) - \langle C(\theta_A)\rangle)(C(\theta_B) - \langle C(\theta_B)\rangle)\rangle$, where $\langle \ldots \rangle$ denotes an ensemble average over experiments and all possible universes. In an ideal experiment, the temperature measured in a pixel is the true sky temperature t_i for a particular manifestation of the CMB fluctuations and n_i is the noise in the measurement, $\sqrt{1/w_i}$. To avoid a profusion of symbols, let $t_i \longrightarrow t_i + n_i, t'_j \longrightarrow t'_j + n'_j$, substitute in $\langle C(\theta_A)\rangle$, and expand fourth order terms with $\langle x_i x'_j x_k x'_l\rangle = \langle x_i x'_j\rangle\langle x_k x'_l\rangle + \langle x_i x_k\rangle\langle x'_j x'_l\rangle + \langle x_i x'_l\rangle\langle x'_j x_k\rangle$, to obtain

$$\begin{aligned}\Sigma_{AB} = \frac{1}{\Gamma_A\Gamma_B} \sum_{i,j\in A;k,l\in B} & w_i w'_j w_k w'_l \Big(\langle t_i t_k\rangle\langle t'_j t'_l\rangle + \langle t_i t'_l\rangle\langle t'_j t_k\rangle \\ & + \langle t_i t_k\rangle\langle n'_j n'_l\rangle + \langle t_i t'_l\rangle\langle n'_j n_k\rangle + \langle t'_j t'_l\rangle\langle n_i n_k\rangle \\ & + \langle t'_j t_k\rangle\langle n_i n'_l\rangle + \langle n_i n_k\rangle\langle n'_j n'_l\rangle + \langle n_i n'_l\rangle\langle n'_j n_k\rangle\Big).\end{aligned} \tag{3}$$

The first two terms in the above expression are the "theory-theory" or "cosmic variance" terms, the next four are the "theory-noise" terms, and the last two are the "noise-noise" terms.

If the noise in the two maps is uncorrelated and the noise within the maps is uncorrelated from bin to bin, as in a cross-correlation, then $\langle n_i n'_j\rangle = 0$ and $\langle n_i n_j\rangle = \delta_{ij}/w_i$, and Equation 3 reduces to

$$\begin{aligned}\Sigma_{AB} = & \frac{1}{\Gamma_A\Gamma_B}\Bigg(\sum_{i,j\in A} w_i w'_j \Big(\sum_{k,l\in B} w_k w'_l \big(\langle t_i t_k\rangle\langle t'_j t'_l\rangle + \langle t_i t'_l\rangle\langle t'_j t_k\rangle\big) \\ & + \sum_{k:j,k\in B} w_k \langle t_i t_k\rangle + \sum_{l:i,l\in B} w'_l \langle t'_j t'_l\rangle\Big)\Bigg) + \frac{\delta_{AB}}{\Gamma_A}.\end{aligned} \tag{4}$$

If the two maps have common values, as in an auto-correlation or when we correlate a map with a subset of the same map, Equation 3 becomes

$$\begin{aligned}\Sigma_{AB} = \frac{1}{\Gamma_A\Gamma_B}\Bigg(&\sum_{i,j\in A} w_i w_j'\Big(\sum_{k,l\in B} w_k w_l'\big(\langle t_i t_k\rangle\langle t_j' t_l'\rangle + \langle t_i t_l'\rangle\langle t_j' t_k\rangle\big)\\ &+ \sum_{k:j,k\in B} w_k\langle t_i t_k\rangle + \sum_{l:i,l\in B} w_l\langle t_j t_l\rangle\Big)\\ &+ \sum_{i\in 1\cap 2} w_i^* \sum_{j,k:i,j\in A;i,k\in B} w_j' w_k\langle t_j' t_k\rangle + \sum_{j\in 1\cap 2} w_j^* \sum_{i,l:i,j\in A;j,l\in B} w_i w_l'\langle t_i t_l'\rangle\Bigg)\\ &+ \frac{\delta_{AB}}{\Gamma_A}\left(1+\frac{\Gamma_A^*}{\Gamma_A}\right).\end{aligned} \tag{5}$$

The differences in (4) and (5) reflect the fact that in a cross-correlation there are twice as many independent pairs of pixels as in an auto-correlation.

As noted above, these expressions are obtained by hypothesizing an ensemble of universes and therefore contain cosmic variance terms. While this is useful for comparing data to models, herein we are concerned only with comparing two data sets, both of which are maps of the same underlying structure. In this case we average not over an ensemble of universes and experiments, but only over an ensemble of experiments. The results are Equations 1 and 2. Note that we are using the measured temperature value of a pixel as an approximation of its true (noiseless) value. This consistently overestimates the diagonal terms of the covariance matrix.

Appendix B: Alternate Derivation Correlation Function Noise Errors

If a map contains only noise, the correlation function is the average of a number of products of temperatures, each of which is drawn from a Gaussian distribution. The probability of getting a certain t_A and t_B within the ranges Δt_A and Δt_B is then

$$D(t_A, t_B)\Delta t_A \Delta t_B = \frac{e^{-t_A^2/2\sigma_A^2}}{\sigma_A\sqrt{2\pi}}\Delta t_A \frac{e^{-t_B^2/2\sigma_B^2}}{\sigma_B\sqrt{2\pi}}\Delta t_B.$$

By transforming such that $v = t_A t_B$, $|u| = t_A^2$ and integrating over u, one can show that $D(t_A t_B) = K_0(|t_A t_B|/\sigma_A\sigma_B)/\pi\sigma_A\sigma_B$ (see Gradshteyn, p. 340), K_0 being a zero-order, modified Bessel function of the second kind.

The distribution of a sum of terms $D(\Sigma_{i=1}^N f_i) = (\sqrt{2\pi})^{N-1} D(f_1) * D(f_2) * D(f_3) * \ldots * D(f_N)$, where $*$ denotes a convolution (see, for example, Butkov). The convolution theorem states that the Fourier transform of the distribution of this sum is

$$\mathcal{F}\{D(\Sigma_{i=1}^N f_i)\}\{k\} = (\sqrt{2\pi})^{N-1}\prod_{i=1}^{N}\mathcal{F}\{D(f_i)\}\{k\},$$

where $\mathcal{F}\{D(f)\}\{k\}$ denotes the Fourier transform of $D(f)$. Thus,

$$\mathcal{F}\{D(\Sigma_{i=1}^N t_{Ai} t_{Bi})\}\{k\} = (\sqrt{2\pi})^{N-1} \prod_{i=1}^{N} \mathcal{F}\Big\{ \frac{1}{\pi \sigma_{Ai} \sigma_{Bi}} K_0 \Big(\frac{|t_{iA} t_{Bi}|}{\sigma_{iA} \sigma_{Bi}} \Big) \Big\}\{k\}.$$

The central limit theorem requires that the convolution of a large number of functions approach a Gaussain. We can write the Fourier transform of this as $\mathcal{F}\{D(\Sigma_{i=1}^N f_i)\}\{k\} = (2\pi)^{-1/2} e^{-k^2\sigma^2/2}$. Recall that multiplying a Gaussian by a constant c changes σ to $c \times \sigma$, and that $\mathcal{F}\{a\pi^{-1} K_0(ax)\}\{k\} = (2\pi(1 + (k/a)^2))^{-1/2}$. We can expand both expressions for the Fourier transform of the sum and, equating terms of second order in k, find that $\sigma = \sqrt{1/\Gamma}$, just the "noise-noise" errors found in Appendix A.

VI. References

Bennett, C. L., *et al.* 1992, ApJ 396, L7

Bond, J. R. 1992, private communication

Bond, J. R. 1993, in preparation

Boughn, *et al.* 1992, ApJ 349, L49

Boulanger, F., 1989, IPAC (Infrared Processing and Analysis Center, CIT), private communication

Butkov, E., *Mathematical Physics*, Addison-Wesley, 1968

Chan, F. K. & O'Neill, E. M., EPRF Technical Report 2-75 (CSC)

Cayón, L., Martínez-González, E., & Sanz, J. L., 1991, MNRAS 253, 599-604

Gradshteyn, I. S., and Ryzhik, I. M., *Table of Integrals, Series, and Products*, Academic Press, Inc. 1980

Kogut, A., et al. 1992, ApJ 401, 1

Meyer, S. S., Cheng, E. S., & Page, L. 1991, ApJ 371, L7

O'Neill, E. M. & Laubscher, R. E., NEPRF Technical Report 3-76 (CSC)

Page, L. A., 1990, MIT PhD. thesis

Page, L. A., Cheng, E. S. & Meyer, S. S. 1990, ApJ 355, L1

Page, L. A., Cheng, E. S. & Meyer, S. S. 1991, Appl. Optics.

Page, L. A., *et al.* 1993, A paper on the radiometer optics, submitted to Applied Optics

Smoot, G. F., *et al.* 1992, ApJ 396, L1

Torres, S., et al. 1989, Data Analysis in Astronomy 1989, Ed. Di Gesù, V., Scarssi, L. & Maccarone, M. C. (New York: Plenum), 319

Wright, E. L., *et al.* 1992, ApJ 396, L13

Figure Captions

Plate 1

The 170 GHz survey data convolved with a 3°.8 Gaussian beam. The map is in galactic coordinates but the galactic center is *not* at the center of the map. A number of gaps in the map due to periodic calibrations have been smeared over by the convolution. The map is binned on the sky in equatorial coordinates with the spherical cube scheme ("CSC format", Chan & O'Neill, O'Neill & Laubscher and Torres, *et al.*, 1989) in $1^\circ.3 \times 1^\circ.3$ pixels, yielding a set of points on the sphere, each with an associated temperature and a statistical weight, $1/\sigma^2$. The total weight, the sum of the individual pixel weights, for $|b| > 15^\circ$ is 0.051 $(\mu\mathrm{K})^{-2}$. The map is not weighted evenly; most of the perceptible variation is due to variation in the weights. The map has greatest sensitivity near the North celestial pole, marked with an 'N', and at a declination of -10°, marked by the lower dotted line. The bright spot at $l \sim 190^\circ, b \sim 10^\circ$ is Jupiter. In the cross-correlation analysis, the data were not smeared, and only data with $|b| > 15^\circ$ is considered. The residual galactic signal at $|b| < 15^\circ$ indicates that the index and/or temperature of the dust for $|b| > 15^\circ$ is different from that of the dust on the plane.

Figure 1

The squares are the cross-correlation between the 170 GHz survey map and the *COBE* DMR 'Fit Technique' reduced galaxy map for $|b| > 15^\circ$. The circles represent the correlation between the masked DMR map and the full-sky DMR map. The 1 σ error bars reflect pure noise only.

Figure 2

The 170 GHz—DMR cross-correlation along with 1 σ distribution of results from simulating and correlating: 1) noise governed by the 170 GHz map weights with noise governed by the DMR map weights, 2) noise governed by the 170 GHz map weights with the real DMR map, 3) simulated $Q_{rms-PS} = 17$ μK Harrison-Zel'dovich skies with 170 GHz weights and noise with the real DMR map, and 4) simulated $Q_{rms-PS} = 17$ μK Harrison-Zel'dovich skies with 170 GHz weights and noise and skies with the same underlying structure and DMR weights and noise. These simulations are intended for qualitative comparison with the data.

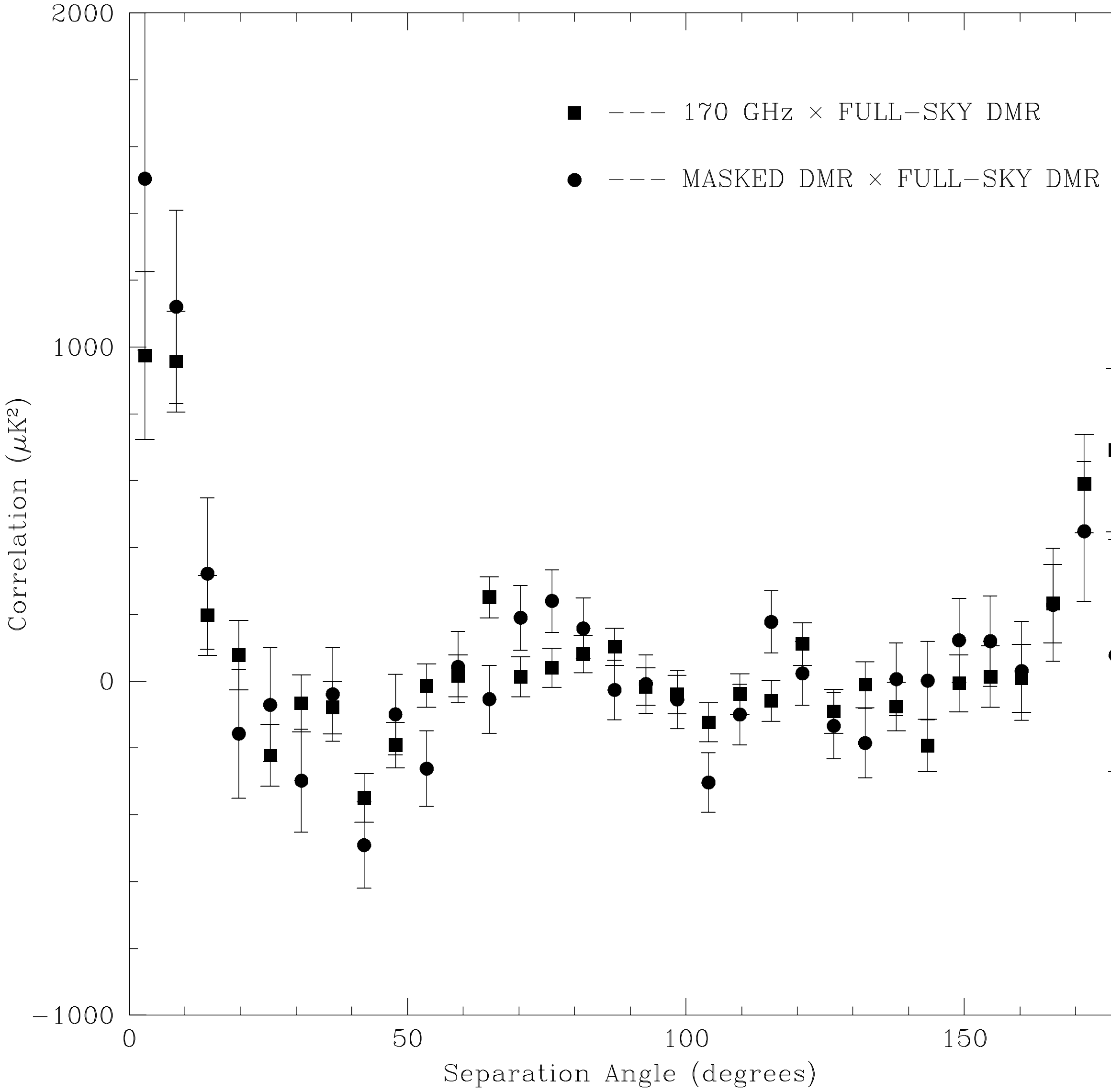

170 GHz × FULL-SKY DMR
MASKED DMR × FULL-SKY DMR
2000
1000
0
−1000
0
50
100
150
Correlation (μK^2)
Separation Angle (degrees)

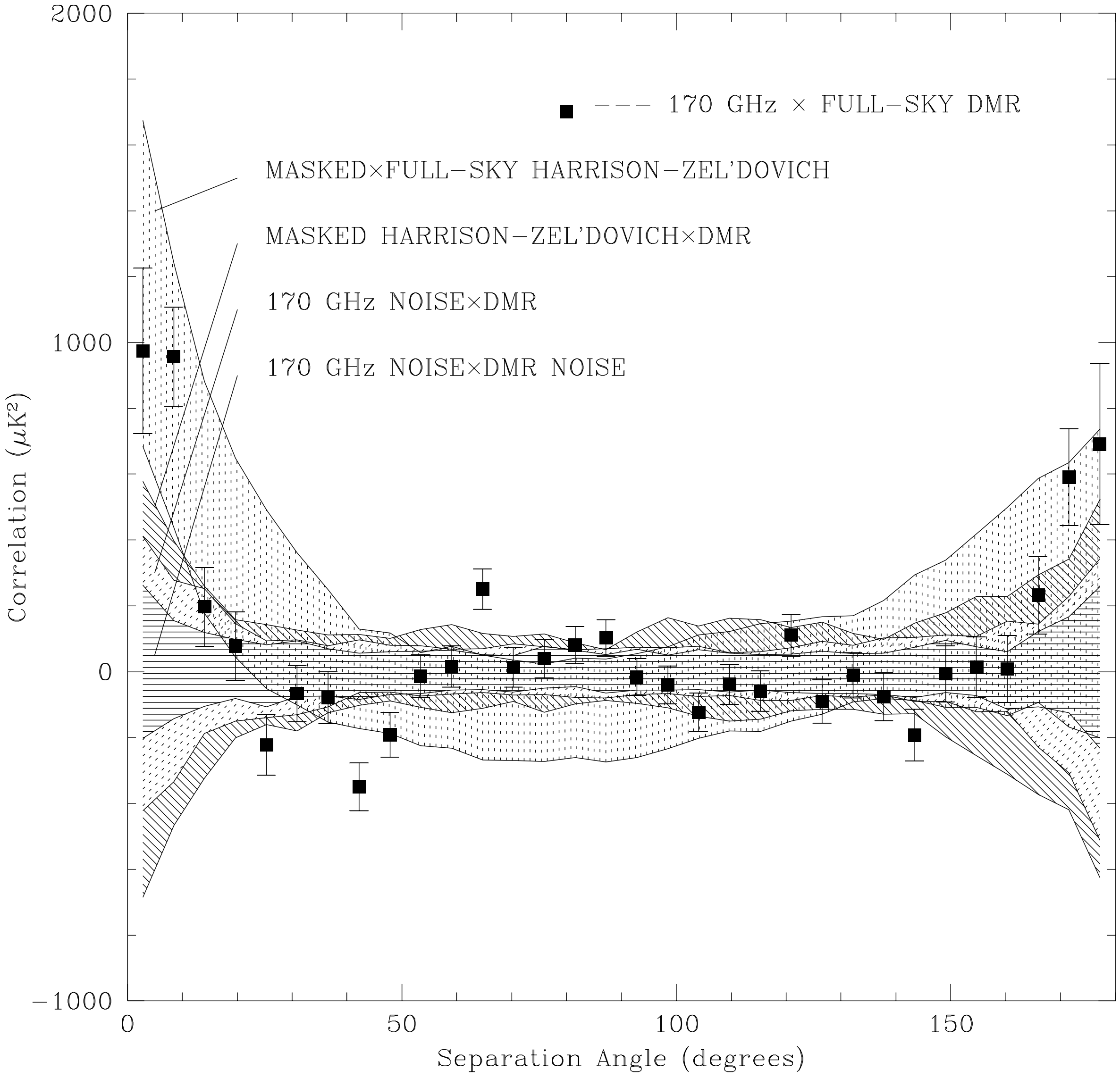

170 GHz × FULL-SKY DMR
MASKED×FULL-SKY HARRISON-ZEL'DOVICH
MASKED HARRISON-ZEL'DOVICH×DMR
170 GHz NOISE×DMR
170 GHz NOISE×DMR NOISE
2000
1000
0
-1000
Correlation (μK²)
0
50
100
150
Separation Angle (degrees)